Scanning Electron Microscopy

Volume 1985 | Number 3 Article 3

8-7-1985

Secondary Ion Mass Spectrometry of Glasses: Aspects of Quantification

H. Odelius
Chalmers University of Technology

A. R. E. Lodding
Chalmers University of Technology

L. O. Werme
Swedish Nuclear Fuel and Waste Management Co.

D. E. Clark
University of Florida

Follow this and additional works at: https://digitalcommons.usu.edu/electron

Part of the Biology Commons

Recommended Citation

Odelius, H.; Lodding, A. R. E.; Werme, L. O.; and Clark, D. E. (1985) "Secondary Ion Mass Spectrometry of Glasses: Aspects of Quantification," *Scanning Electron Microscopy*: Vol. 1985 : No. 3 , Article 3.
Available at: https://digitalcommons.usu.edu/electron/vol1985/iss3/3

This Article is brought to you for free and open access by the Western Dairy Center at DigitalCommons@USU. It has been accepted for inclusion in Scanning Electron Microscopy by an authorized administrator of DigitalCommons@USU. For more information, please contact digitalcommons@usu.edu.

SCANNING ELECTRON MICROSCOPY/1985/III (Pages 927-934)
SEM Inc., AMF O'Hare (Chicago), IL 60666-0507 USA

0586-5581/85$1.00+.05

SECONDARY ION MASS SPECTROMETRY OF GLASSES: ASPECTS OF QUANTIFICATION

H. Odelius, A.R.E. Lodding+, L.O. Werme§ and D.E. Clark§§

Physics Department, Chalmers University of Technology, Gothenburg, Sweden
Swedish Nuclear Fuel and Waste Management Co., Stockholm, Sweden§
Department of Materials Science and Engineering, University of Florida§§

(Paper received March 16, 1985: manuscript received August 07, 1985)

Abstract

SIMS routines have been developed for the analysis of oxide materials, with applications particularly in element profiling of corrosion layers on glasses after weathering or leaching. The possibilities of quantification and reproducibility have been found critically sensitive to the build-up of charge on the insulating specimens. With control of constant specimen potential, relative sensitivity factors in the positive mass spectrum have been determined for about 20 elements in 10 different alkali-borosilicate glasses. Secondary ion yields were studied as functions of the energy range of ions admitted to the analyzer. At relatively low energies, including the top of the energy distribution, the formalism of the "local thermal equilibrium" model was found to be very well approximated, strongly favoring the yields of elements with low ionization potentials. For ions with relatively high energies the role of E_i was less pronounced, and there were some indications of atomic binding effects.

With well-defined conditions of energy pass window and of offset in sample voltage, considerable reproducibility of calibration could be obtained. In routine profiling it has been found advantageous to work at rather high offset, which rendered a narrowed range of specific elemental yields, easily interpreted mass spectra, and reduced sensitivity to surface charge effects.

KEY WORDS: Secondary ion mass spectrometry; sputtering; ion emission; quantification; element profiling; glasses; insulators; ionic energy distributions.

+Address for correspondence:
A.R.E. Lodding, Physics Department, Chalmers University of Technology, S-41296 Göteborg, Sweden.

Phone No. (46-31) 810100

Introduction

It is known /11, 7/ that oxide materials exhibit relatively (compared to, e.g., metals) high yields of positive ions on sputtering. For this reason, and also because the amorphous state gives freedom from crystallographic and granular effects, glasses have been relatively frequently studied by secondary ion mass spectrometry (SIMS). Indeed, standard glasses have been extensively employed in "round robin" type investigations /13, 14/. However, until recently the scatter of results from different laboratories has been considerable, even when instruments of the same type were used. This indicated a need of continued investigation into the mechanisms of secondary ion emission.

Improved SIMS instrumentation, together with close attention to experimental details, has in recent years brought sufficient reproducibility to permit efficient and quantitative measurements of element concentrations in glasses, particularly of in-depth distributions in near-surface regions such as corrosion layers. Most published work has been performed on nuclear waste borosilicate glasses containing a range of simulated fission products /2, 4-6, 8, 9, 17/. A similar SIMS technique has also been applied to glasses of archeological interest /15/.

The chief impediments to reproducibility and quantification in such measurements have been seen to be linked with the insulating nature of glass. The build-up of a surface charge from impingent primary ions and from the emission of secondary electrons tended to change the effective potential of the sputtered specimen during profiling, causing the energy distribution of the secondary ions to drift past the energy acceptance "window" of the analyzer. The control of this tendency, together with care in the definition of the admitted energy range, has been necessary for obtaining meaningful results.

The object of the present paper is a) to present the newly determined SIMS sensitivity factors for some 20 elements in ten alkali borosilicate glasses; and b) to review and discuss the systematics of quantification in these glasses, with particular regard to the energy distributions of the secondary ions.

Experimental

The compositions of the ten glasses are listed in Table 1. They were developed primarily for the purpose of a systematic leaching investigation /2/. They may be seen to vary mainly in respect of the proportions of the alkalis, boron, iron, zinc and silicon. In regard of corrosion and wear properties, they have been found to exhibit considerable differences.

The smooth (1 μm grade polish) surfaces of the glass specimens were coated with a 100 nm gold layer in order to reduce charging effects in SIMS analysis. In the quantification study and in the latest profiling work /2/, "second generation" commercial SIMS equipment was used (Cameca IMS-3F with a Hewlett-Packard minicomputer). The specimens were sputtered either with defocused O_2^+ (ca 5 keV), utilizing an electron gun for surface charge neutralization, or with a relatively narrow beam of O^- (ca 15 keV). Steady secondary ion emmission could be achieved in both procedures, but for routine profiling the latter was adopted, offering simpler offset control and faster, easily adjusted erosion rate. The consumption rates of the ten glasses were between ca 100 and 500 $(\mu m^3)/\mu As$. The actual rate of sputtering was varied between ca 0.3 and 30 μm/h, by control of the primary current (0.05 - 1 μA) and/or the bombarded area (50x50 - 350x350 μm^2). For optimal in-depth resolution the analyzed area was always considerably less than that of the crater bottom. After each completed profile the mean sputter rate was found by measurement of the crater depth with a stylus-type surface level monitor (Rank Talysurf). In cases where several corrosion levels of different sputter characteristics were to be traversed, successive profiles were taken to different depths. The calculated sputter rate in each layer was fed into the computer to calibrate the depth scale in the final profile evaluation.

Only positive ion emission was studied, as hitherto it has not been possible routinely to maintain a sufficiently steady emission in the negative spectrum.

The concentration profiles were recorded cyclically, with pre-selected adjustments of the magnet field corresponding to successive mass numbers, normally 24 per cycle. The duration of a cycle was of the order of two minutes. At the beginning of each cycle the computer was programmed to correct the sample potential by seeking a given reference mass peak. Although the ion currents of different elements were recorded at different times within each cycle, in the final evaluation the computer effected an interpolation between successive readings for each mass, relating to a common real time in the cycle for purposes of final quantification.

Figs. 1 a,b show a typical primary plot (in counts/s versus sputtering time) of in-depth profiles of ions of different mass numbers across a corroded near-surface layer of a glass after a standard leaching test. Figs. 2 a,b give the corresponding profiles after final evaluation, with account taken of differential sputtering rates and of elemental sensitivity factors. The latter (obtained as discussed in the following section) were used by the computer to convert relative ion counts into relative molar concentrations. These values, from all cation elements of appreciable concentrations, were added up to 100% to yield the "absolute" concentrations on the ordinate axis.

The "dV" curve in the raw data plot shows the gradual increase of sample voltage compensation with the growth of surface charge. No steady emission of secondary ions could be maintained without such compensation.

For the profiles in figs. 1 and 2, the secondary ions were admitted for analysis within the energy pass window of 100 eV and with an offset in sample potential of -60 V. The analyzer accepted, under these circumstances, ions with energy increments betwen ca 40 and 140 eV (see fig.3 below). The elimination of the secondary ions at the low energy end of the energy range naturally reduces the detector signal (e.g., by ca two powers of ten for Si^+). At the concentrations of relevance in the present study, viz., ca 4 ppm or higher, this is unimportant compared to the following advantages: a) The intensity of molecular peaks is considerably suppressed (see, e.g., the 44-SiO^+ curve in fig.3); at the conditions of this investigation, none of the peaks used for analysis (of more than 20 elements) had a molecular background exceeding some 1% of the monatomic peak. b) The reproducibility is improved; as the slope of the energy distribution at the edge of the window is only moderate, the readings are relatively unaffected by small changes in sample potential. c) Because the most easily ionized elements exhibit the steepest drop at the low energy end of the distribution (see fig.3 below), the dynamic range necessary for the collector is reduced to experimentally realistic limits (within ca 7 orders of magnitude, see figs.1).

As has just been seen, a knowledge of the energy distributions was essential for the choice of practical experimental conditions. The curves in fig.3 were obtained on an uncorroded bulk glass specimen using a "sliding" energy window of 0.5 eV with an O^- primary beam of ca 1 μA. In the diagram the ordinates were adjusted to make the curves coincide at their maxima.

Results and Discussion

A glance at fig.3 suffices to demonstrate that the relative ion yields of different elements must be sensitively dependent on the position and width of the energy pass window. In Table 1 the secondary ion signals, normalized to that of 28-Si^+, are listed for 10 standard glasses, as recorded under the normal analyzing conditions, viz., 100 eV window, -60 V offset. These normalized values represent the averages of results obtained for each standard glass by one profile at low depth (ca 0 - 0.3 μm) in the uncorroded specimen, and the deep end (well beyond the corroded zone) of at least one profile in the leached glass. No significant depth dependence of these relative yields could be noticed.

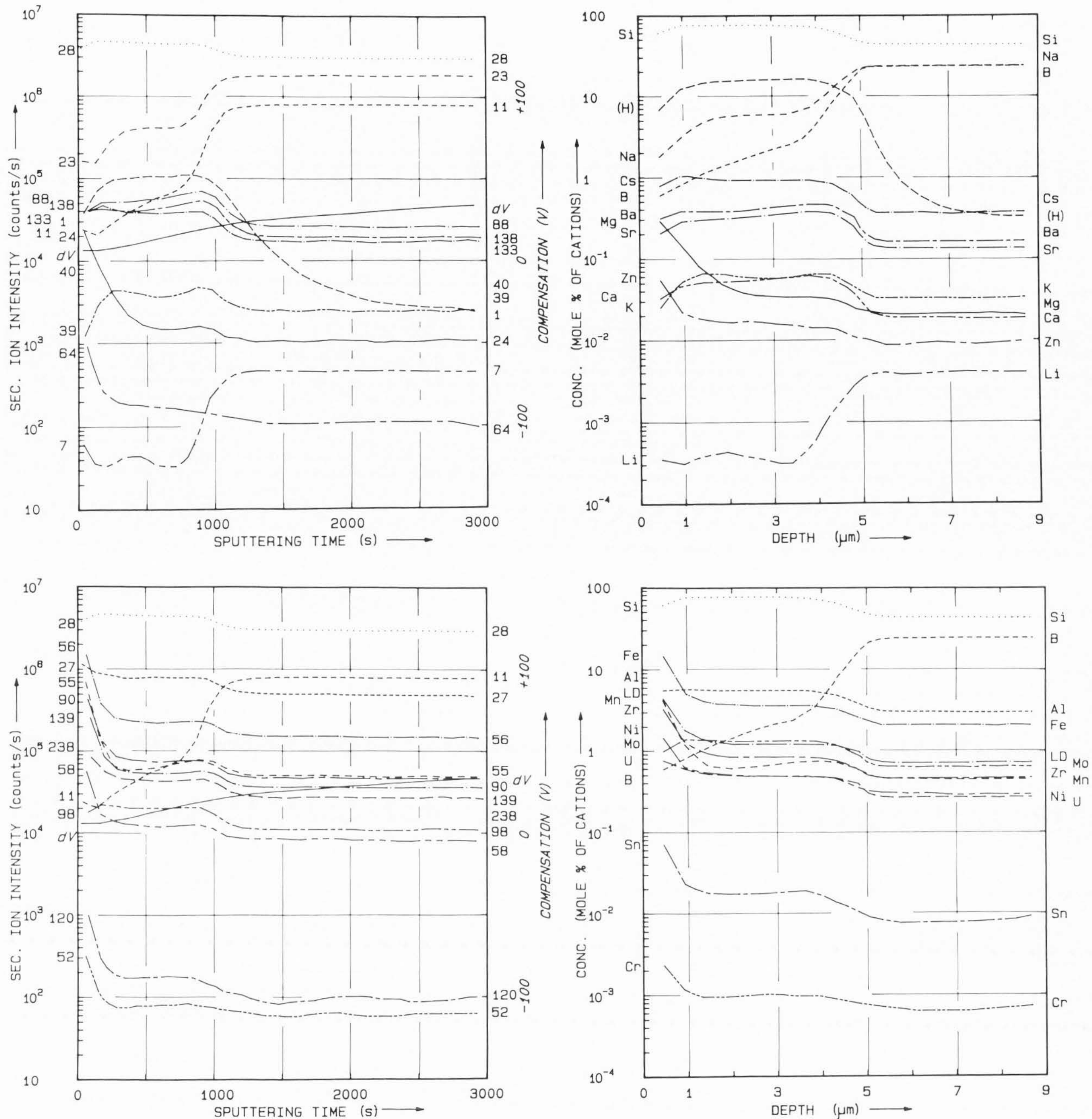

Figures 1 and 2: SIMS in-depth profiles of elements after 28 days leaching.

Figure 1 (Left): Raw data (ion counts versus time). dV (on a linear scale): voltage compensation for surface charge build-up.

Figure 2 (Right): Processed data (mole percent of total cations, except hydrogen, versus depth).

Upper diagrams: Group I and II elements, Si and B.

Lower diagrams: Group III and IV elements, transition metals. LD: all lanthanides and yttrium.

Recorded at 100 eV energy window, -60 V h.v. offset.

Table 1. Cation compositions of ten ABS glasses. Isotope secondary ion yields. Calibration factors. For symbols, see eqs. 1 a,b in text. Recorded at energy pass range 100 eV, offset -60 V.

Glass	L	Si	Li	Na	Cs	Ca	Sr	Ba	Zn	B	Al	Y	La	Sn	U	Cr	Mn	Fe	Ni	Zr	Mo
	I	28	7	23	133	40	88	138	64	11	27	89	139	120	238	52	55	56	58	90	98
ABS 39	Mole %	40.8		21.0	0.32		0.13	0.15		29.0	3.07	0.08	0.22	0.006	0.32		0.45	3.60	0.25	0.54	0.57
	i_{IL}/i_{28}	1.0		0.7	0.006		0.008	.007		0.29	.21	0.005	.013	0.00004	.0075		0.016	0.095	0.003	0.017	0.004
	CF	1.0		1.36	.77		2.75	1.90		0.43	2.80	2.9	2.38	0.23	0.95		1.45	1.08	0.48	1.31	0.29
ABS 41	Mole %	42.6	9.8	15.2	0.31		0.12	0.15	1.85	22.7	2.40	0.07	0.21	0.006	0.31		0.44	1.85	0.24	0.52	0.55
	i_{IL}/i_{28}	1.0	0.37	0.48	.0060		0.008	.0065	.007	0.22	.145	.0055	.013	0.000035	.0080		0.0015	.041	0.0019	.016	0.004
	CF	1.0	1.60	1.35	.83		2.80	1.90	0.165	.414	2.59	3.2	2.55	0.25	1.10		1.55	0.95	0.33	1.31	0.31
ABS 118	Mole %	38.8	6.5	16.3	0.40	3.69	0.16	0.19	1.60	20.6	4.95	0.10	0.28	0.008	0.16	0.34	0.57	1.86	0.60	1.08	0.72
	i_{IL}/i_{28}	1.0	0.28	0.51	.008	.35	0.01	0.009	.010	0.22	.30	0.008	.019	.00004	.0043	.014	.022	0.052	0.0054	.033	0.04
	CF	1.0	1.68	1.21	.81	4.67	2.50	1.75	0.255	0.4	2.34	3.1	2.60	0.23	1.05	1.55	1.70	1.08	0.36	1.18	0.20
EXP 1	Mole %	47.3		16.8	0.33		0.13	0.16	2.00	25.25	2.63	0.08	0.23	0.006	0.326		0.47	2.04	0.26	0.56	0.595
	i_{IL}/i_{28}	1.0		0.41	.0065		0.0075	.006	0.008	.205	.135	0.006	.012	0.00003	.0065		0.017	0.0475	.0029	.0155	.0025
	CF	1.0		1.15	.93		2.65	1.85	0.19	0.39	2.37	3.7	2.45	0.24	0.90		1.70	1.10	0.52	1.31	0.20
EXP 2	Mole %	44.4		20.8	0.32		0.13	0.15	1.9	23.65	2.50	0.075	.225	.006	0.317		0.46	1.92	0.255	0.54	0.58
	i_{IL}/i_{28}	1.0		0.62	.0055		0.008	.0065	.012	0.205	.175	0.006	.012	0.000035	0.0072		0.016	0.0475	.0026	.015	0.004
	CF	1.0		1.33	.76		2.75	1.90	0.28	.305	3.12	3.4	2.40	0.24	1.00		1.65	1.10	0.46	1.23	0.30
EXP 3	Mole %	42.7	9.8	15.15	.30		0.12	0.14		22.8	2.42	0.07	0.21	0.006	0.298		0.425	1.84	0.235	0.50	0.54
	i_{IL}/i_{28}	1.0	0.37	0.48	.0042		0.0085	.0072		0.20	.17	0.005	.014	0.000035	0.0075		0.017	0.051	0.0025	.017	0.004
	CF	1.0	1.60	1.35	.60		3.05	2.15		0.38	2.98	3.0	2.85	0.24	1.05		1.70	1.19	0.45	1.45	0.33
EXP 4	Mole %	39.9		20.7	0.32		0.13	0.15	1.9	27.2	3.02	0.075	.225	.006	0.317		0.46	3.52	0.255	0.545	0.58
	i_{IL}/i_{28}	1.0		0.65	.0075		0.0095	.007	0.012	.27	.205	.006	.014	.00004	.007		0.019	0.100	0.0036	.0175	.004
	CF	1.0		1.26	.93		2.95	1.85	0.255	0.395	2.70	3.1	2.50	0.27	0.85		1.75	1.10	0.56	1.35	0.29
EXP 5	Mole %	44.15		21.4	0.325		0.13	0.155		23.8	2.51	0.075	.23	0.006	0.326		0.46	3.66	0.255	0.545	0.58
	i_{IL}/i_{28}	1.0		0.71	.0072		0.0085	.0067		0.23	.22	0.006	.012	0.000035	0.0075		0.0175	.100	0.0033	.015	0.0035
	CF	1.0		1.46	.99		2.95	1.90		0.425	3.10	3.3	2.35	0.24	1.05		1.65	1.20	0.57	1.25	0.28
EXP 6	Mole %	42.8		20.9	0.32		0.125	.15		27.6	3.05	0.075	.22	0.006	0.317		0.45	1.88	0.25	0.53	0.565
	i_{IL}/i_{28}	1.0		0.63	.0060		0.0085	.0065		0.265	.17	0.005	.012	0.00003	.008		0.017	0.049	0.0026	.016	0.004
	CF	1.0		1.29	.81		2.85	1.85		0.41	2.39	2.8	2.30	0.24	1.05		1.60	1.11	0.44	1.33	0.29
EXP 7	Mole %	39.4	9.8	15.55	.31		0.125	.145		26.75	2.96	0.072	.215	.006	0.307		0.435	3.47	0.245	0.515	0.55
	i_{IL}/i_{28}	1.0	0.41	0.59	.0085		0.0095	.0075		0.27	.195	.0055	.125	0.000035	.0085		0.018	0.098	0.0028	.017	0.0035
	CF	1.0	1.65	1.49	1.05		3.05	2.00		0.40	2.60	2.9	2.30	0.23	1.10		1.65	1.11	0.45	1.31	0.25
CF (mean)		1.0	1.63	1.325	0.85	4.65	2.83	1.91	0.23	0.404	2.70	3.15	2.47	0.24	1.01	1.55	1.64	1.102	0.46	1.30	0.27
S.D.			0.04	0.11	.13		0.18	0.11	0.05	0.02	.30	0.30	0.17	0.02	0.09		0.09	0.068	0.08	0.08	0.05

A comparison with the mole concentrations in the respective glasses, also listed in Table 1, yields the "isotopic" calibration factors, defined as

$$(CF)_{IL} = \frac{i_{IL}/i_{28}}{c_L/c_{Si}} \qquad (1a)$$

where i_{IL} denotes the measured ion current of isotope I of element L, and c is the respective molar concentration of the elements. As seen in Table 1, the scatter of the CF values for each element is quite moderate within the whole range of ten investigated alkali borosilicate glasses. The mean values and standard deviations (S.D.) are given at the end of Table 1.

Table 2 lists the measured relative sensitivity factors,

$$(RSF)_L = \frac{b_{28}}{b_{IL}}(CF)_{IL} = \frac{i_L/i_{Si}}{c_L/c_{Si}} \qquad (1b)$$

where b is the respective isotopic abundance. The RSF factors are listed here for different ranges in the energy distribution. The first column corresponds approximately to a narrow energy range at the very top of the distribution. It is obvious that the RSF values may change very much on moving from the first column to the second or third, but that they level out at high offsets to become more or less constant. This is in line with

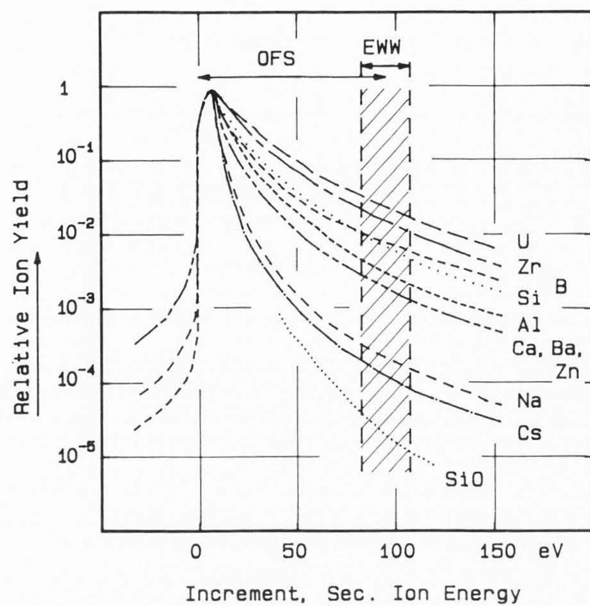

Figure 3. Energy distributions of secondary ions from an alkali borosilicate glass sputtered with 15 kV O^- ions. Vertical axis adjusted for all profiles to coincide at the maximum. The energy pass window EWW and the sample voltage offset OFS are here illustrated at arbitrary values.

other recently published work /12/, exploiting some of the advantages of analysis at high energy offset. One may also notice in Table 2 that the RSF values of the listed elements range through more than two powers of ten at low ion energies, but that at high offsets the sensitivities are all practically in the same order of magnitude.

In addition to the elements listed in Table 2 quantification has also been attempted in regard of oxygen and hydrogen. The $18\text{-}O^+$ signal was generally quite low and showed considerable scatter. For H, no exact standards have yet been obtained, and although reproducibility was reasonable, systematic errors could not be excluded. It should be mentioned here, however, that with 100 eV energy window and -60 V offset the elemental sensitivity factors (RSF) with respect to silicon were found to be of the order of 4×10^{-3} for oxygen and 9×10^{-2} for hydrogen (with an uncertainty factor of ca 3 for the former, ca 2 for the latter). Because of their high ionization potentials (see below) the ion yields of these elements were very sensitively affected even by very small changes in analytical conditions.

Currently no theory of the ionization mechanism of sputtering has been accepted as both quantitative and rigorous. It is, however, often worth while to discuss the elemental systematics of ion yields in terms of the so-called LTE ("local thermal equilibrium" /1/) formalism. For a number of matrices, an expression of the form

$$i_L/c_L = (\text{const.})\, M_L^{-n}(B/B_0)_L \exp(-E_{iL}/kT) \qquad (2)$$

Table 2. Relative sensitivity factors (RSF, normalized to Si) of elements at different ranges of secondary ion energy distribution. MAX: at top of distribution. EWW: width of energy pass window (in eV). OFS: offset in sample potential (in -V). Si_{abs}: intensity of Si^+ signal, relative to top of distribution.

EWW / OFS	Max	25 / 10	25 / 20	25 / 40	25 / 80	100 / 60
Li	9	2.6	1.7	1.35	1.2	1.62 ± 0.04
Na	33	3.0	1.9	1.2	0.95	1.22 ± 0.11
Cs	40	3.9	1.55	0.75	0.55	0.78 ± 0.15
Ca	14	5.6	4.8	4.3	4.1	4.4
Sr	8.9	4.0	3.3	2.8	2.5	3.15 ± 0.20
Ba	7.0	3.5	2.7	2.05	1.8	2.15 ± 0.12
Zn	0.95	0.48	0.38	0.36	0.35	0.41 ± 0.10
B	0.50	0.43	0.42	0.45	0.52	0.455 ± 0.02
Al	4.0	3.1	2.6	2.2	2.0	2.50 ± 0.28
Y						2.9 ± 0.35
La	1.7	1.9	1.95	2.0	2.2	2.4 ± 0.25
Sn						0.59 ± 0.05
U	0.35	0.55	0.7	0.9	1.0	0.84 ± 0.08
Cr						1.7
Mn	3.0	1.8	1.6	1.3	1.2	1.51 ± 0.08
Fe	2.8	1.7	1.3	1.05	0.85	1.11 ± 0.07
Ni	1.2	0.65	0.5	0.45	0.45	0.63 ± 0.12
Zr	1.4	1.75	1.85	1.95	2.0	2.30 ± 0.15
Mo	0.7	0.75	0.8	0.85	0.9	1.10 ± 0.25
Si_{abs}	1	1/8	1/25	1/100	1/400	1/50

has been found to give at least a reasonable approximation /7/. Here M_L is the atomic mass of element L; the exponent n is frequently assumed /13/ to be 0.5; B/B_0 is the ratio of the thermodynamic partition functions (that of the singly ionized state to that of the ground state of the atom /3/); E_i is the first ionization potential; and T_i is an entity usually called "ionization temperature", typical of the matrix. Usually T_i has been found to be of the order of 5000 K in metals, 10000 K in oxides /7/.

In fig.4, the results of the present quantification work are expressed as

$$\Gamma_{rel} = (i_L/c_L)(M_L/_{Si})^{0.5}\frac{(B/B_0)_{Si}}{(B/B_0)_L} \qquad (3)$$

and plotted against E_i. All points are seen to conform qualitatively to the requirements of eq.2. The points represented with rings are based on the yields of secondary ions at "low" energies, i.e., at the top of the energy distribution. For nearly all the elements, from the alkalis on the left to hydrogen and oxygen on the right, the

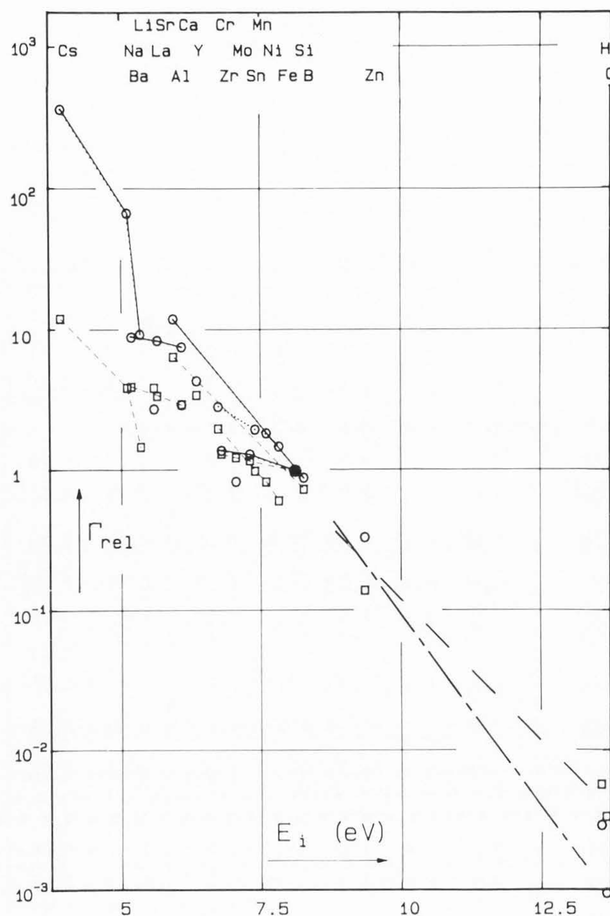

Figure 4. Specific ionic emissivities (normalised to Si^+) of elements in SIMS, plotted vs first ionization potential. For definition of Γ_{rel}, see equation 3.
Rings: ions at top of energy distribution.
Squares: ions within an energy pass window of 100 eV with -60 V offset in sample potential.

points are seen to lie more or less along a straight line, the slope of which yields an "ionization temperature" of the order of 8500 K. The agreement is of course to some extent conditioned by the arbitrary assumption of n=0.5 in eq.2. This has been qualitatively supported by isotope measurements for Li and Si in glasses /16/, but actually a range of different n values has been reported for elements in different matrices /10/. E.g., for the Sn isotopes in tin metal it has been found with good reproducibility /16/ that n lies well above 1.5, while the boron isotopes in silicon implied n to be less than unity. Careful studies of the mass dependence of the ion emission in SIMS at present offer particular promise to penetrate the intricacies of the ionization mechanism. It is possible that a higher n value than 0.5 may apply for relatively heavy elements. If so, the agreement with the LTE formalism would, on the whole, be even better than in fig. 4.

The points marked as squares in fig.4 show the systematics as obtained with the actually employed practical routines. i.e., with an energy pass window of 100 eV and an offset of -60 V. Here the Γ_{rel} values of the elements on the LHS of the diagram are seen to be considerably lowered. The straight line approximation still appears reasonable, yielding T_i in the order of 12500 K. However, some tendencies imply that the mechanism at relatively high offset may be dependent not exclusively on E_i, but also on the binding in the matrix.

Thus, for the monovalent elements (Cs, Na, Li, possibly H) the points are seen to lie somewhat below the other systematics. The divalent elements (Ba, Sr, Ca, Zn) also fall well below the mean straight line. The trivalent ones (Al, B) lie higher, but still below the tetravalent Si.

Avoiding at this stage getting involved in speculation, one may nevertheless point out that, from the point of view of a pair-splitting model, the ionization probability for a cation in an oxide might be considered to be proportional to the number of its oxygen bonds. If, in fig.4, particularly in regard of the points marked with squares, the values for the alkalis are multiplied by 4, those for the divalent ions by 2, and those for the trivalent ones by 4/3, a "better" straight line is certainly obtained.

Thus it is implied, from a comparison in fig.4 of the systematics of "squares" with that with "rings", that a) the effective "ionization temperature" increases with the kinetic energy of emerging secondary ions; and b) the ion yield, especially at the high energy tail of the distribution, may be significantly affected by binding parameters such as valency, oxidation state, or coordination number.

Conclusion

A reproducible and efficient procedure has been developed for quantitative SIMS analysis of glasses. Sensitivity factors, established for more than twenty elements, are found to vary in strong dependence on the energy of the ions admitted to the analyzer. In the systematics of elemental ionization yields, the first ionization potential is seen to play a major role, but there are also signs of differential influences from atomic binding parameters in the glass lattice.

Acknowledgement

We are indebted to the Swedish Nuclear Fuel and Waste Management Co. for financial support to glass making and analysis, as well as for important travel grants (DEC, AREL).

References

/1/ Andersen CA, Hinthorne JR (1973). Thermodynamic approach to the quantitative interpretation of sputtered mass spectra. Analyt.Chem. 45, 1421-1438.
/2/ Clark DE, Lodding ARE, Odelius H, Werme LO (1985). Element profiling by SIMS of surface lay-

ers in glasses. Microchim.Acta, in press.
/3/ De Galan L, Smith R, Winefordner JD (1968). The electronic partition functions of atoms and ions between 1500 and 7000 K. Spectrosc.Acta 23B, 521-524.
/4/ Hench LL, Werme LO, Lodding A (1982). Burial effects on nuclear waste glass. In: Scientific Basis of Nuclear Waste Management; W. Lutze (ed), North-Holland, NY, 153-162.
/5/ Hench LL, Lodding A, Werme LO (1984). Analysis of one-year in-situ burial of nuclear waste glasses in Stripa. Adv.Ceramics 8, 310-323.
/6/ Hench LL, Lodding A, Werme LO (1984). Nuclear waste glass interfaces after one year burial in mine environment; glass-glass interfaces. J.Nucl.Materials 125, 273-279.
/7/ Lodding A (1982). Trends and developments in secondary ion mass spectrometry for microanalysis. In: Euranalysis IV, Revs. on Analyt.Chem.; L.Niinistö (ed), Akademiai Kiadö, Budapest, 75-103.
/8/ Lodding A, Odelius H (1983). Applications of SIMS in interdisciplinary materials characterization. Microchim.Acta Suppl.10, 21-49.
/9/ Lodding A, Hench LL, Werme LO (1984). Nuclear waste glass after one year burial; glass-bentonite interfaces. J.Nucl.Materials 125, 280-286.
/10/ Lorin JC, Havette A, Slodzian G (1982). Isotope effects in secondary ion emission. In: SIMS III; A.Benninghoven, J.Giver, J.Laszlo, M.Riedel, H.W.Werner (eds). Springer Ser.Chem.Phys. 19, 115-123.
/11/ McHugh JA (1975). Secondary ion mass spectrometry. In: Methods of Surface Analysis; S.P.Wolski, A.W.Czanderna (eds), Elsevier, Amsterdam, 223-278.
/12/ Metson JB, Bancroft GM, McIntyre NS, Chauvin WJ (1984). Molecular ion suppression in the secondary ion mass spectra of minerals. In: SIMS IV; A.Benninghoven, J.Okano, R.Shimizu, H.W.Werner (eds), Springer Ser.Chem.Phys. 36, 466-468.
/13/ Morgan AE (1980). An alternative to the relative sensitivity factor approach to quantitative SIMS analysis. Surf. & Interf.Anal. 2, 123-133.
/14/ Newbury DE (1979). Instrumental effects on quantitative analysis by secondary ion mass spectrometry. In: SIMS II; A.Benninghoven, C.A.Evans, R.A.Powell, R.Shimizu, H.A.Storms (eds). Springer Ser.Chem.Phys. 9, 53-57.
/15/ Schreiner M, Stingeder G, Grasserbauer M (1984). Quantitative characterization of surface layers on corroded medieval window glass with SIMS. Fres.Z.Analyt.Chem. 319, 600.
/16/ Södervall U, Odelius H, Lodding A (1985). SIMS studies of self-diffusion and of associated isotope effects. Springer Ser.Chem.Phys, in press.
/17/ Werme LO, Hench LL, Nogues J-L, Odelius H, Lodding A (1983). On the pH-dependence of leaching of nuclear waste glasses. J.Nucl.Materials 116, 69-77.

Discussion with Reviewers

D.S.Simons: What was a typical difference in sputter rate between leached and non-leached zones in a glass?
Authors: In the investigation reported in ref./2/ the mean erosion rate in the leached layers exceeded that in the bulk by a factor 1.9 ± 0.5.

D.S.Simons: Why was the erosion rate faster for O^- than for O_2^+ when the maximum current density for the latter is much higher than for the former?
N.S.McIntyre: Would you comment on the use of the electron gun as an effective neutralizing source when using an O_2^+ primary ion beam?
Authors: In order to cope with the surface charge caused by the positive oxygen bombardment, the ion beam had to be very considerably defocused. However, rastering over a large area was not desirable, as a large opening in the Au coating impaired the efficiency of charge removal. Hence, the current density of O_2^+ had to be kept much lower than achievable. With the use of an electron gun it is usually found that complete neutralization is hard to reach in practice. The compensation of dV is not simple to effectuate and, in order to achieve a homogeneous image, slow sputtering rates are necessitated. E.g., an Atomica ion probe at Zürich, capable of similar ion densities as available in the present study, and equipped with a considerably more sophisticated electron gun, when working with positive oxygen beam for the analysis of glasses arrives at sputtering rates lower by a factor of 3 to 10 than those reported in the present paper.

D.S.Simons: Is there any physical significance to the position, relative to sample potential, of the energy distributions?
Authors: The position is mainly given by the surface charge build-up and by the automatic compensation of dV. The curves in fig.3 are all recorded at relatively great penetration depth in bulk glass at one set value of primary ion current and raster.

J.B.Metson: The reproducibility in the change in charge compensation (dV in fig.1) is of interest. The reproducibility is good for the glasses analyzed. Do the authors find much variation with other matrices and conditions?
Authors: Differences between different insulators are relatively minor in this respect, compared to the effects of the density and raster of the primary beam, particularly the area of the sputtered crater. E.g., at given primary current in the present investigation, a raster of 250x250 μm^2 causes typically a twice or three times faster rise in dV than does 50x50 μm^2, and the approached maximum in dV is considerably higher.

J.B.Metson: What relationship do the authors anticipate between the exponent n in the mass ratio (LTE formalism) and agreement with LTE? Is there any physical justification for varying n with mass?
Authors: A priori, of course, no such relationship may be anticipated as long as the LTE model does not stand on a more rigorous theoretical basis than to-day. However, empirically it is indeed implied that n may vary with M even within a given matrix, and attempts have been made to interpret this physically (see, e.g., ref./10/).

D.S.Simons: Do you have any evidence to show that the Relative Sensitivity Factors remain the same in the leached zone of the glass where B and Na are quite depleted and H is enriched w.r.t. bulk?

Authors: This important point has been subject to some study in our laboratory. Relatively extensive leached portions of selected glasses have been analyzed wet-chemically and by electron probe as well as by SIMS. With reservation for the crudeness of the complementary techniques (only the 4 to 6 major constituent elements could be studied) the indications are that the differences of the obtained RSF values from those in bulk glass are marginal, in the sense that the effective "ionization temperature", T_i in the LTE formalism, differs by less than ca 15 percent from that in the bulk glass.